EJARS Egyptian Journal of Archaeological and Restoration Studies "EJARS"
An International peer-reviewed journal published bi-annually

Volume 6, Issue 2, December - 2016: pp: 71-84
www. ejars.sohag-univ.edu.eg

Original article

THERMAL DEGRADATION OF PAPER: THE STRUCTURAL CHANGES OF FIBRES

Hassan, R.
Conservation dept., Faculty of Archaeology, Cairo Univ., Cairo, Egypt.

E-mail: *rusdyarabii@yahoo.com*

Received 5/7/2016 Accepted 21/11/2016

Abstract

The current study reported the thermal degradation behavior of three paper fibers; cotton, mechanical& sulfite wood pulp, exposed to dry-heat ageing ate150 °C,130 °C and 105 °C for one month. The structural changes of fibers were evaluated by SEM, infrared spectroscopy (FTIR) study and X-Ray Diffraction (XRD). SEM data show that the chemical pulp is more resistant to heat ageing than the cotton and mechanical pulp in the early stages. Dramatic changes in functional groups on the paper surface, as monitored by infrared spectroscopy, occurred in the samples before and after ageing. The FTIR results indicated that an elimination of the band at "amorphous & crystalline" regions under thermal ageing was occurred.

Keywords: *Thermal degradation, Crystallinity index, Cellulose, FTIR, Wood pulp*.

1. Introduction

Cellulose is the most abundant renewable polymer on Earth, with many attractive physical and chemical properties including biocompatibility, biodegradeability, hydrophilicity, stereoregularity, reactive hydroxyl groups and ability to form suprastructures [1, 2]. The cellulose chain bristles with polar -OH groups, these groups form many hydrogen bonds with OH groups on adjacent chains, bundling the chains together. The chains also pack regularly in places to form hard, stable crystalline regions that give the bundled chains even more stability and strength. Cellulose has a strong tendency to form intra- and inter-molecular hydrogen bonds by the hydroxyl groups on these linear cellulose chains, which stiffen the straight chain and promote aggregation into a crystal-lline structure 3 and give cellulose a multitude of partially crystalline fiber structures and morphologies [3-5]. A major part of our cultural heritage has been recorded in various forms on paper for centuries [6]. The preservation of historical objects is the main aim of museums and other institutions, which take care of historical objects. Cultural heritage objects are subject to the influence of environmental parameters, e.g., light, temperature, and moisture, which cause different structural changes on the materials. The long term exposure to variable conditions changes the structure and properties of the materials. As a result of ageing (mechanical and photochemical damage) the fibres become more susceptible to bio deterioration [7, 8]. Moreover, developing an understanding of the causes and mechanisms of cellulose degradation has been the subject of substantial research over the past 50 years. Its effects are well documented: old books, textiles, or paper insulation can undergo brittle failure after years, decades, or even centuries of service. Some materials withstand ageing better than others which suggest that sample chemistry is central to the degradation process. In order to model long-term changes in a manageable time scale, accelerated ageing is used. By the use of elevated temperature, changes which might require years or decades to occur under normal service conditions can be achieved using much shorter time scales [9]. Paper fibres have several important characteristics, which determine their structural and mechanical properties. The fibre wall thickness, the fibre collapsibility and the degree of fibrillation are just a few examples of the characteristics that describe a fibre structure and behavior [10, 11]. When cellulosic materials are exposed to elevated temperatures, changes can occur in their chemical structures that affect its performance. The extent of the changes depends on the temperature level and the length of time under exposure conditions. The changes in chemical structure may be manifested only as reduced strength, and hydroscopic water. In contrast, very drastic chemical changes may result in reduced strength and significant carbohydrate weight loss. Heat plays a major rule in paper degradation, heat has ageing effect on paper and over long period can do considerable damage to it .In general, it can be stated that exposure to high temperature [12]. Thermal decomposition of paper and other cellulosic materials was widely studied in the literature [13]. A key mode of cellulose degradation involves the disintegration of supra molecular structures formed by hydrogen bonds between OH-groups, considered as the major factor controlling the structure and the physical property of cellulose [14]. Thermal ageing changes the surface charge of fibres which are supposed to be due to pH changes of aged pulp fibres or/and the degradation of the paper. The acids are located in the whole volume of the pulp fibre wall and can influence the fibre surface pH. Changes in pH can vary the surface charge by influencing the functional group dissociation. It is known that the negative charge of pulp fibres decreases with the lowering of pH [15]. Moreover, the hornification process is one of closing (impermeability) the structure of cellulose fibres to water due to irreversible hydrogen bond formation between the micro-fibrils and other structural units of cellulose fibres. The size of pores is reduced, the structure of paper becomes more compact, and the paper becomes significantly more brittle. After ageing, the wet structure resembles more closely a dry one, suggesting that water cannot expand the structure to the same extent. It is postulated that an increase in local ordering of ageing creates a structure more resistant to disruption by water, thermal degradation of cellulosic materials is greater in present of air than in its absent, because of oxidation by atmospheric oxygen. Furthermore, thermal degradation is greater under steaming than under dry heating conditions. The activation energies for the degradation reactions are about half as large as under dry heating conditions [16]. Also, the large numbers of specific reactions and products involved in the thermal degradation of cellulose have been the subject of extensive studies. Mechanisms and Kinetics remain controversial, but it has been established that the first step in cellulose degradation is the production of laevoglucose which either decomposes to volatile fragments, or reacts further to produce [17, 18]. On the other hand, it is known that the mechanical properties of paper decrease during accelerated ageing because the degradation of paper is associated with the formation of low molecular products such as formic, acetic and lactic acids, among others. The formation of these acids leads to a self-promoting hydrolytic degradation chain reaction, or auto-catalysis [19, 20]. The influence of the oxidation process results in the formation and release of degradation products containing a carbonyl group (C=O) and double bond (C=C) .However, no researches were conducted to study and evaluate the changes in the structural morphology of paper degraded by heat. So, the present study, based on SEM examination, seeks to illustrate the morphological and structural changes of the paper decayed by heat and its deterioration potential in air which is essential for understanding the aging of paper cultural heritage objects and for knowing the proper procedures to conserve them.

2. Materials and Methods

2.1. *Materials*

Paper samples used were purified cotton linter cellulose ($40 g/m^2$), mechanical wood ($40 g/m^2$) pulp & bleached sulfite wood pulp ($40 g/m^2$). The prepare paper sheets were used according to Swedish standard method (SCA), pulps were beaten to 40◦ SR in a Jokro mill beater. Besides a paper sheet delivered from Rakta (paper mill-Alexandria).

2.2. *Accelerated ageing*

In order to model the long-term degradation processes in an appropriate time scale, the paper samples were exposed to accelerated-ageing procedures. The dry-heat ageing (RH= 0) at 150° C, 130 °C and 105 °C, respectively, was performed according to ISO5630-1 [21-23] for 30 days.

2.3. *Investigation methods*

2.3.1. Scanning electron microscopy (SEM)

Specimens for this study were cut from the samples. Specimen size was 10 mm diameter and it was circular in shape. These samples subjected to sputter coating (Edwards's model S 140 A) of gold ions to have a conducting medium. Sputter coated samples were scanned with JEOL Model JSM-T20 SEM.

2.3.2. FTIR

The samples were analyzed before and after ageing with a FTIR spectrometer (Model 6100 Jasco, Japan). Each spectra was obtained in the transmission mode with TGS detector and by using KBr method and represents (2 mm/s) co -added scans at the spectral region ranging from 4000 to 400 cm^{-1} with resolution of 4 cm^{-1}.

2.3.3. X-ray diffraction (XRD)

The band positions of crystalline and amorphous cellulose forms of untreated & treated samples were measured by using a Philips Analytical X-Ray B.V.; PCAPD diffraction software; diffract meter type: PW 1840, with a Cu tube anode; generator tension 40kV and generator current 25 mA. The Cu Kα radiation consisted of Kα1 (0.154056nm) and Kα 2 (0.154439nm) components. Scans were obtained from 5 to 30 degrees 2θ in 0.03 degree steps for 0.3 seconds per step. The crystallinity index (CI) was calculated according to the method of Segal et al, i.e. ((I002_ I18)/I002) X100, with the diffraction intensities, I002 at002 peak position (2θ ≈ 22.5º) and I18 at 2θ = 18º (amorphous) [24, 25].

3. Results

3.1. *Scanning Electron Microscopy*

As shown in fig$_s$. (1-8) with the absence of heat, the fibrous structure of paper morphology was apparently normal; paper surface was smooth with optimal pore sizes. It can be observed that the linkage with the model paper is very close. Moreover, the well organized network of fibrils covering the fibre surface can easily be visualized.

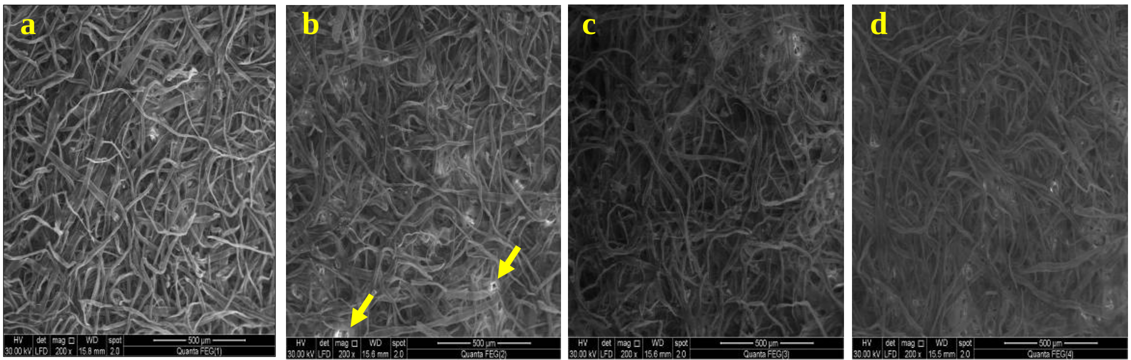

Figure (1) Shows SEM micrographs of aged cotton paper, showing surface morphology after one month, **a**. control paper (bar 500 µm), **b**. at 105 ˚C (bar 500 µm), **c**. at 130 ˚C (bar 500 µm), **d**. at 150 ˚C (bar 500 µm) ,the arrows refer to the new pores after ageing at 105ºC

3.1.1. Aged cotton paper

SEM micrographs of the surface confirmed the formation of small cracks in some areas on the cotton fibres, fig$_s$. (2b, 3b), in addition to the pores, which are formed in the surface of fibres after 1 month of heat ageing at 105 °C. Starting from130 °C the small cracks penetrated between cell walls, fig$_s$. (2-c, 3-c). SEM micrographs of surfaces heat-treated paper revealed the formation of different patterns of fibres cracks due to heat treatment and artificial ageing. The difference in paper surface structure can cause decayed differences between paper surfaces, but this was almost unnoticed in the tangential section, fig. (4-a). At 150 °C shrinkage penetrated between cell walls and the decay was apparent and the surface of the paper was uneven; damaged fibres induced by heat show irregular and bleb-like protrusions on their surfaces. The cells became shrunken after heat action. The micrographs showed diff-erences in paper degradation patterns between different temputures under this study. The results proved that at 150 ˚C the cotton fibres have hornifcation. These results indicated that in order to achieve hornifcation, some, but not necessarily all, water must be removed. This can be done by wet pressing, drying in a desiccator at room temperature, or by drying the sample in an oven. Higher temperature serves two distinct roles: first, it increases the rate of evaporation, and secondly it increases molecular mobility. Without molecular mobility, structural rearrang-ements such as those proposed by Christensen (1966) [26].

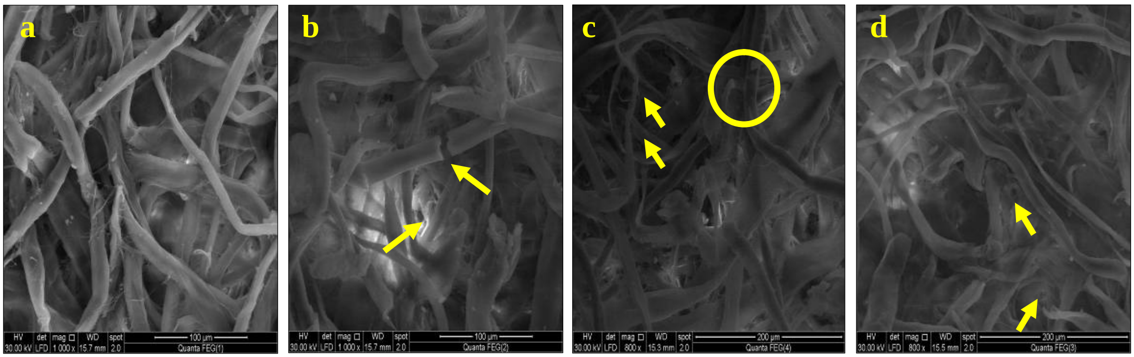

Figure (2) Shows SEM micrographs of aged cotton paper, showing surface morphology after one month, **a**. control paper (bar 100 µm), **b**. at 105 ˚C (bar 100 µm), **c**. at 130 ˚C (bar 200 µm), **d**. at 150 ˚C (bar 200 µm) the arrows refer to the cutting in the fibers.

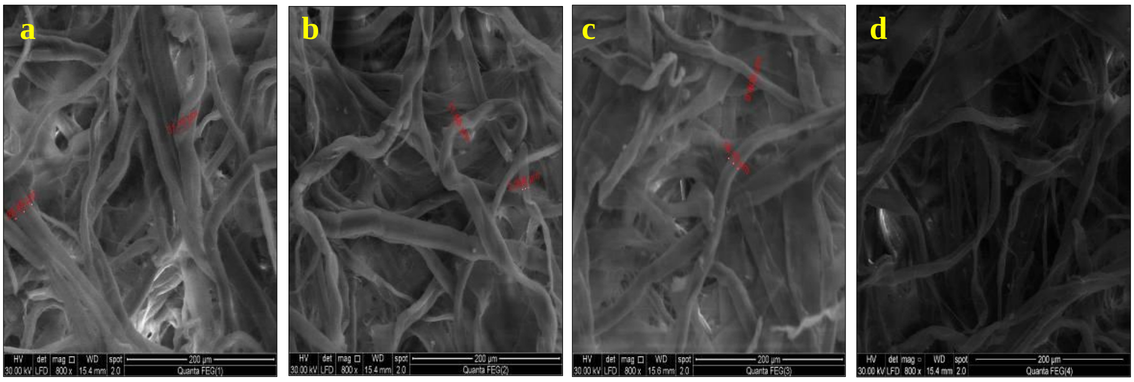

Figure (3) Shows SEM micrographs of shrinkage of cotton fibres on a string structure:, showing size of fibres after one month of heat ageing, **a**. control paper (bar 200 µm), **b**. at 105 ˚C (bar 200 µm), **c**. at 130 ˚C (bar 200 µm), **d**. at 150 ˚C (bar 200 µm).

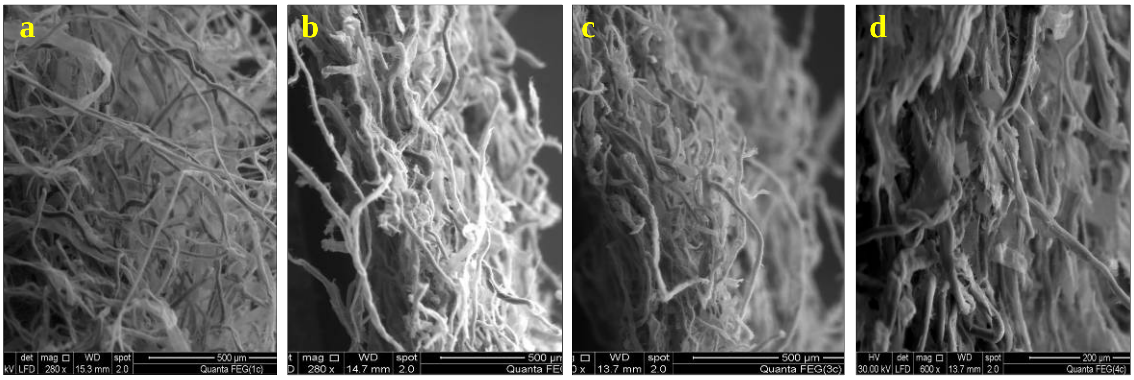

Figure (4) Shows SEM micrographs of cross section in cotton paper, showing shape of cotton fibres after one month of heat ageing, **a**. control paper (bar 500 µm), **b**. at 105 ˚C (bar 500 µm), **c**. at 130 ˚C (bar 500 µm), **d**. at 150 ˚C (bar 200 µm).

3.1.2. Aged mechanical wood paper

Microscopic examination of aged paper at 105 ˚C showed erosion of the fibres wall in some areas, fig$_{s}$. (5-b, 6-b). Moreover, the micrographs (5-c, 6-c) showed that the degradation was evident at 130 ˚C as fibres gradually became more disrupted. At 150 ˚C advanced stage of decay was observed since the micro fibrils wall layers are disrupted and dispersed due to the extensive attack on the walls. The overall effect is that the paper loses its strength; during our studies we have observed fibre fragments in the form of what we call a “volatile fragments” structure, fig$_{s}$. (5-d, 6-d).

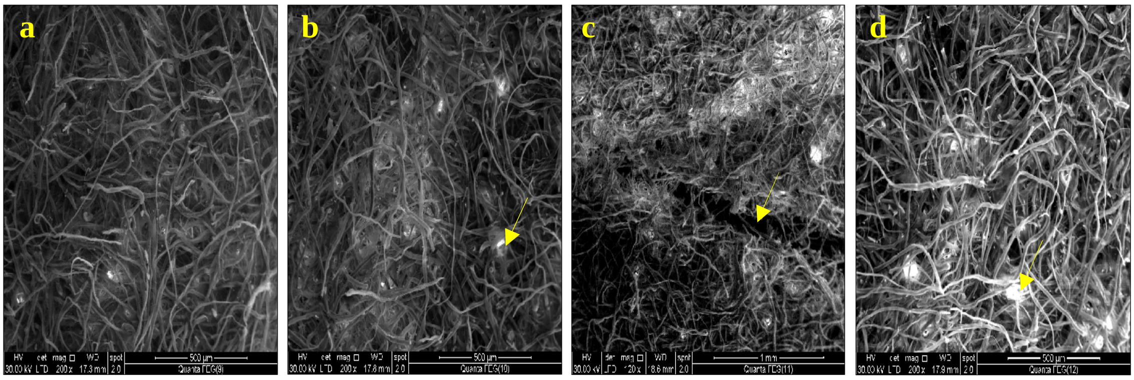

Figure (5) Shows SEM micrographs of aged mechanical wood pulp, showing surface morphology after one month, **a**. control ((bar 500 µm), **b**. at 105 ˚C (bar 500 µm), **c**. at 130 ˚C (bar 500 µm), **d**. at 150 ˚C (bar 500 µm) ,the arrows refer to the formation of small cracks.

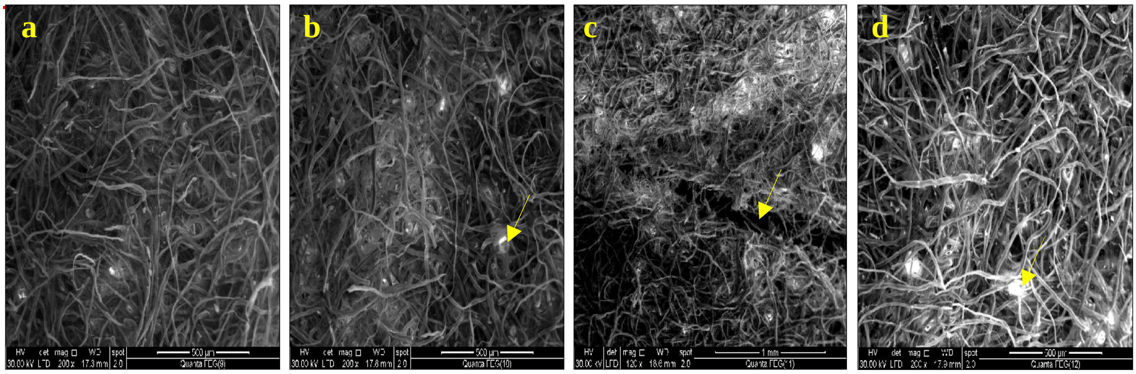

Figure (6) Shows SEM micrographs of aged mechanical wood pulp, showing fibres fragments in the form of what we call a “volatile fragments” structure separations and fractures between cell walls were observed **c**. (bar 200 µm), **d**. (bar 200 µm).

3.1.3. Aged chemical wood pulp

Some fibres or bundles split and wind up and turn into thinner fibres after 1 month of heat ageing at 105 °C, fig$_{s}$. (7-b, 8-a). At 130 °C, a profile similar to a shrinkage activity profile of a fibre sample with initial increasing activity was seen, fig$_{s}$. (7-c, 8-b), high activity in the main shrinkage interval where the largest population of fibres shrinks exhibited significant changes in their surface characteristics. The width of some fibreile decrease to 17.62 µm as comparison of reference paper. At 150 ˚C, wood pulp fibres disintegrate into characteristic fragments. It seems that cellulose in the various cell wall layers has been degraded. Consequently, separation between two adjacent cells occurred and the fibres loosened, collapsed, and became detached from the substrate of paper .Moreover cracks were formed on the surfaces of fibres after artificial ageing.

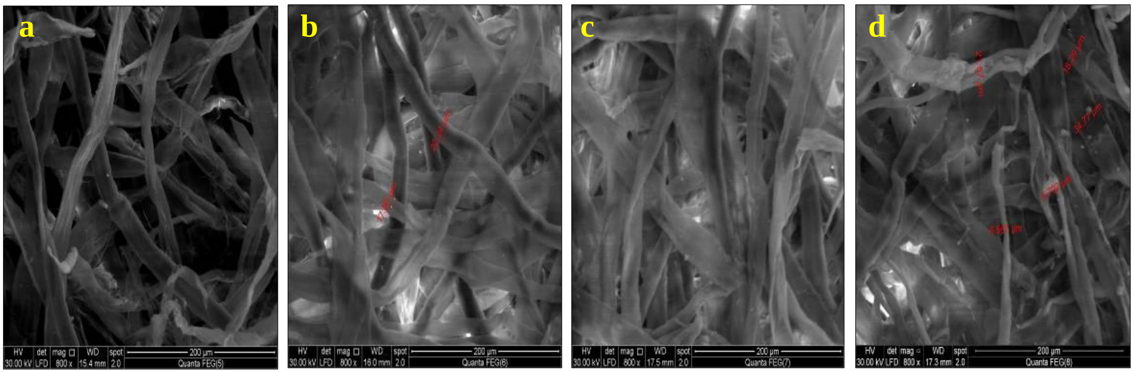

Figure (7) Shows SEM micrographs of aged chemical pulp, showing surface morphology after one month, **a**. control paper (bar 200 µm), **b**. at 105˚C (bar 200 µm), **c**. at 130˚C (bar 200 µm), **d**. at 150˚C (bar 200 µm).

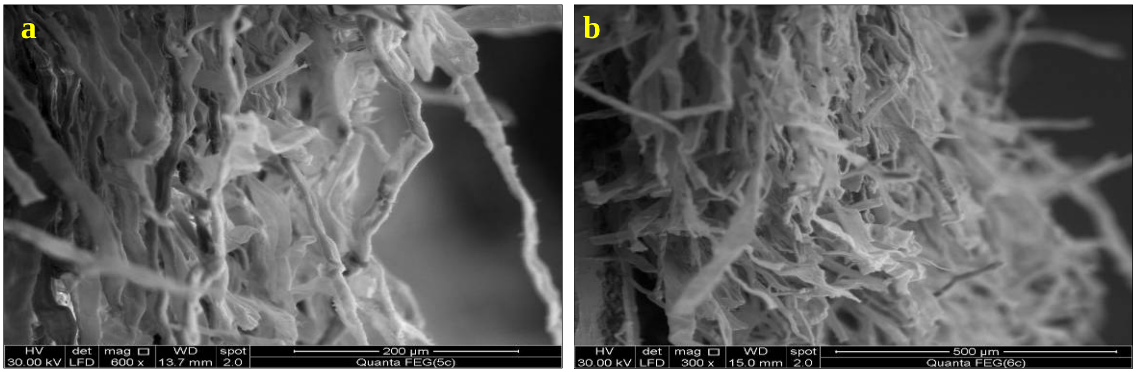

Figure (8) Shows SEM micrographs of cross section in chemical pulp, **a**. control paper (bar 200 µm), **b**. at 105˚C (bar 200 µm) showing that the fibre exhibiting generalized thinning and erosion of the cell walls leading to breakdown of the paper cells which became easily fragmented.

3.2. *FTIR spectra of paper samples exposed to accelerated ageing*

Paper samples were studied by FTIR spectroscopy before and after heat ageing and results were compared to monitor changes**.**

3.2.1. Un aged paper

The infrared spectra of paper show the same basic structure as all paper samples [27-29], as assigned in tab. (1). The relative intensities of bands at 3439 and 1069 cm-^{1} are higher in the cotton, whereas bands at 1635.34, 1454, 1159 and 778 cm-^{1} are stronger in chemical pulp. The higher cellulose content in chemical pulp than mechanical pulp results in a stronger asym. Out of phase ring stretching band at 877 cm-^{1}. In addition, there are many peaks in the fingerprint region between 1800 and 600 cm-^{1} in wood pulp paper. The peaks in the fingerprint were assigned [30-32], 1483 cm-^{1} and 1454 cm-^{1} for asymmetric bending in CH3, 1375 cm-^{1} for C–H deformation in cellulose and hemicellulose, 1330=1320 cm-^{1} for C–H vibration in cellulose and Cl–O vibration in syringyl derivatives, 1158 cm-^{1} for C–O–C vibration in cellulose and hemicellulose, 1159 cm-^{1} for aromatic skeletal and C–O stretch, 1069 cm-^{1}for C–O stretch in cellulose and hemicellulose and 876 cm-^{1}for C–H deformation in cellulose.

Table (1) the functional groups in paper.

Wave number cm-^{1}	**Functional group**
3400-3409cm-^{1}	Very strong, broad hydrogen bonded (O-H) stretching absorption
2894.7cm-^{1}	C-H stretching due to aromatic and symmetric stretching
1650 cm-^{1}	O-H bending band
1545 cm-^{1}	O-H str. first overtone(intermolecular H-bond), cellulose
1457 cm-^{1}	O-H str. first overtone, cellulose
1107,1053.8,1031 cm-^{1}	C - O stretching vibration
895-899 cm-^{1}	C-H deformation in cellulose.

3.2.2. Aged paper

FTIR spectra of paper samples exposed to 105 °C, 130 °C & 150 °C for one month are shown in fig$_{s}$. (9-11) respectively. Significant changes in IR spectra can be seen at very early stages of decay in all samples

3.2.2.1. *Aged cotton paper*

No dramatic changes are observed before and after ageing at 105 ˚C, fig. (9), but it is interesting to note that after ageing there are some differrences in the decrease of the relative intensity of the O-H group at 3400 cm-^{1} and change the shape of the peak may be an indication of the increase the rate of evaporation, and secondly it increases molecular mobility. The other fingerprint bands remain somewhat similar to that seen for the control sample except new band at 900.5, 1160.94 &1111.76 cm-^{1} appeared (in comparison to the untreated sample). It may be due to C–O group of ester formation or new C–OH groups resulting from opening of the pyranose ring. More carbonyl groups were formed as a result of further oxidation of C–OH groups' cellulose molecules [33] and there has been the removal of the association CH stretching, where the oxidation process of cellulose to occur where heat oxidized hydroxyl group cellulose molecule to the carbonyl and carboxyl group [34]. On the other hand, at 130 ˚C a small shift in the expected OH stretching and C-H stretching due to aromatic and symmetric stretching at 3413.39 and 2901.38, respectively.

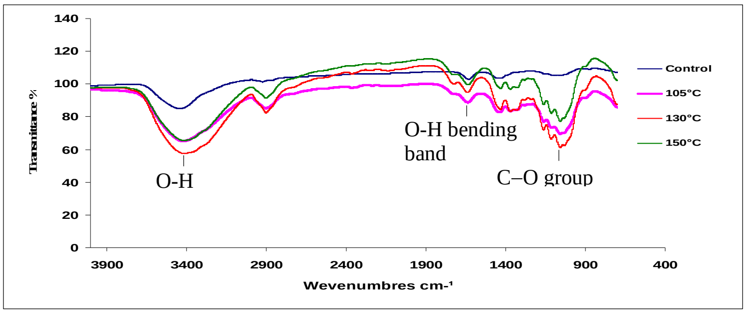

Figure (9) Shows comparison of four spectra scanned in transmittance, cotton reference and thermo deteriorated cotton specimen: Bands at 3439, 1635and 1058 cm-^{1} are marked.

3.2.2.2. *Aged mechanical pulp*

The ageing studies of mechanical pulp in the laboratory, in air at 105 ˚C, showed an increase in absorbance in the FTIR spectrum in the region of 1600-1700 cm-^{1}. However, the changes were masked by sample to sample variation, due to the presence of an O-H stretch from free water in the paper near 1700 cm-^{1}. This peak can be shifted to lower wavelength if the water is replaced by O_2 and the development of the ageing peak at about 1710 cm-^{1} is then be clearly seen, as shown in fig. (3), In addition, the 876 cm-^{1} bands which represent the C-H stretch third overtone have disappeared. The intensity of the carboxylic peak near1600 cm-^{1} also increases with ageing, fig. (10). The actual peak heights vary slightly with position on the surface of the sample, due to local in homogeneity of the surface of the paper. Moreover, dramatic changes are observed before and after ageing at 130 ˚C, the presence of a new very strong peak with maximum at 1372 & 1333 cm-^{1}. The new bands can be attributed to the 2 x C-H str. +C-H deformation, cellulose & Isolated O-H str. first overtone, respectively. At 150 ˚C, it is interesting to note that here are some differences in the decrease of the relative intensity of the C-H deformation, cellulose at1337 cm-^{1}. The other fingerprint bands remain somewhat similar to that seen for the aged paper at 130 ˚C. A shoulder at 1267 cm-^{1}, which was not observed in the spectrum of un decayed paper, develops in the band at 1230 cm-^{1}. It has been shown that the guaiacyl type (softwood lignin) absorbs near 1268 and 1230 cm-^{1} and that the syringyl type (the major type of paper lignin) absorbs only at 1230 cm-^{1}. Although paper lignin also contains guaiacyl moieties, the absorption band at 1268 cm-^{1} may have been supper-ssed by a strong absorption at 1230 cm-^{1}. The appearance of the 1268 cm-^{1} band in decayed mechanical pulp may be mainly due to decrease in the intensity of 1230 cm-^{1} band resulting from xylan degradation, since this band results partially from the C–O in xylan. Significant changes in IR spectra confirmed that higher temperature serves two distinct roles: first, it increases the rate of evaporation, and secondly, it increases molecular mobility. Without molecular mobility, structural rearrang-ements such as those proposed by several authors [35,36].

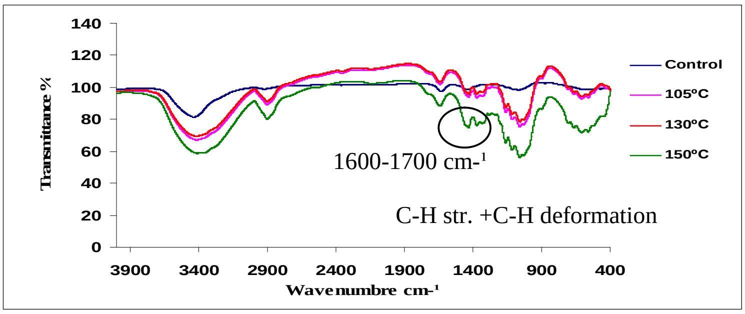

Figure (10) Shows comparison of four spectra scanned in transmittance, mechanical pulp reference and thermo deteriorated wood pulp specimen. Bands 1372 & 1333 cm-^{1} are marked

3.2.2.3. *Aged chemical pulp*

In the case of chemical pulp at 105 ˚C, fig. (11), the intensities of C-H deformation in lignin and carbohydrates bands at 1159, 1330 and 1454 cm-^{1} decrease with exposure time to the heat. At 130 ˚C, it is interesting to note that here are some differences in the decrease of the relative intensity of 1096, 1454, 1636 cm^{1} with those at 778 and 2369 cm-^{1} almost absent after one month exposure. In contrast, intensities of absorption bands resulting from lignin at 1596, 1505, 1462, 1425, 1330, 1244 and 1122 cm-^{1} increases as decay progresses. The current study proved that differences between spectra of degraded and modern paper fibres have been investigated especially the differences in the regions, which are characteristic of crystalline and amorphous cellulose which is indicative for the changes in the fibre structure. The mechanical behaviour of pulp cellulose samples reduction of the band at 900 cm-^{1} which characterized of the amorphous cellulose is observed. In addition, there are observed correlation between different temperature and redu-ction of the band intensity at 900 cm-^{1}. Thus the changes in amorphous region must have been caused by heat. Broadening of this band reflects larger amount of amorphous structure. Its absorbance is notable increased by mercerization as well, when the crystalline structure changes from cellulose I to cellulose II [37-41].

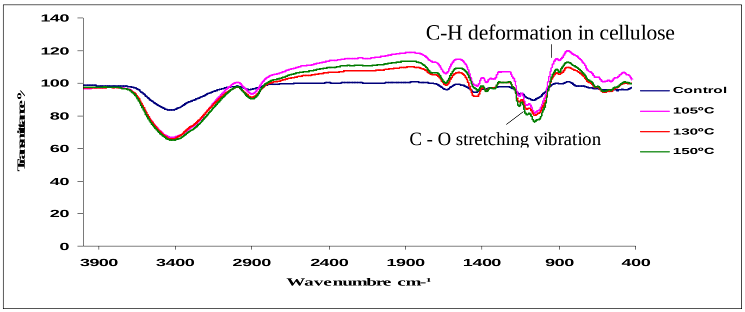

Figure (11) Shows comparison of four spectra scanned in transmittance, chemical pulp reference and thermo deteriorated wood pulp specimen. Bands at 895,899 and 1122 cm-^{1} are marked

3.3. *Cellulose Crystallinity*

Cellulose molecules are strongly associated through inters and intermolecular hydrogen-bonding and Vander Waals forces that result in the formation of micro fibrils, which in turn form fibers. Cellulose molecules are oriented in parallel, with reducing ends of adjacent glycol chains located at the same end of a micro fibril. These molecules form highly ordered crystalline domains interspersed by more disordered amorphous regions. The degree of crystallinity in native cellulose is 60-90 % [42]. The crystalline part of native cellulose is thought to be a mixture of two crystalline modifications, cellulose Iα and cellulose Iβ [43, 44]. X-ray diffraction is a method used generally to evaluate the degree of crystallinity in several materials. Among paper, only cellulose is crystalline, while hemicellulose and lignin are non-crystalline [45]. Consequently, the use of crystallinity as an index of structural change in dried or thermally-aged fibres may not yield clear conclusions. As shown in fig$_{s}$. (12, 13, 14), the X-ray diffractograms of the paper samples studied. In order to examine the intensities of the diffraction bands, establish the crystalline and amorphous areas. The peak intensities and peak broadening differ from one species to another. The more pronounced difference occurs at the peak range between 22.5 2θ and 22.6 2θ reflection assigned with a crystallographic plane of cellulose, as can be seen in tab. (2), where, the rigidity of cellulose fibers increases and their flexibility decreases with increasing ratio of crystalline to amorphous regions at 105 ˚C higher than 130 &150 ˚C

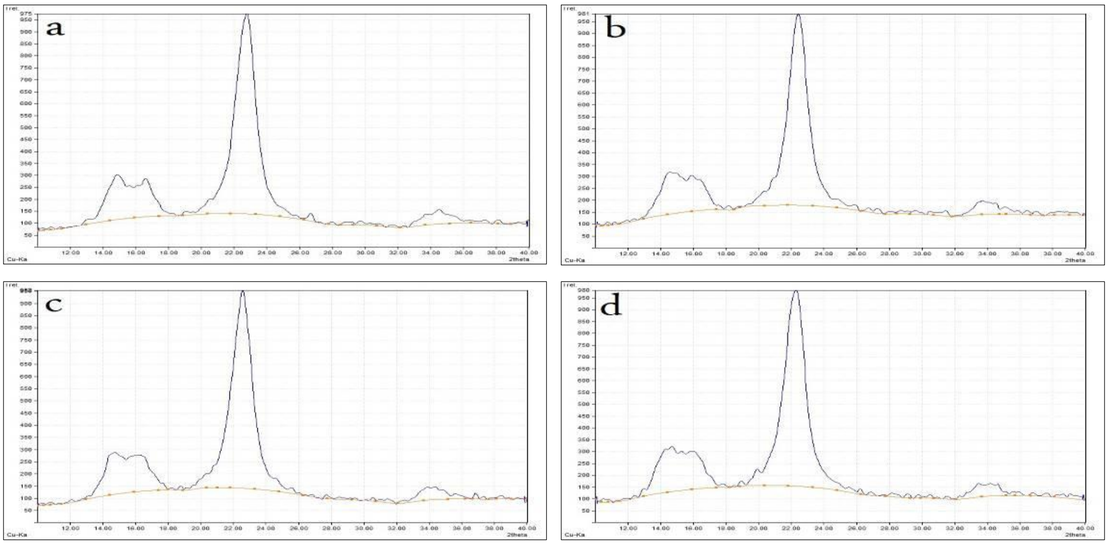

Figure (12) Shows X-ray diffractograms of cotton paper studied before and after ageing , (a) control, (b) aged at 105 ˚C, (c) aged at 130 ˚C & (d) at 150 ˚C

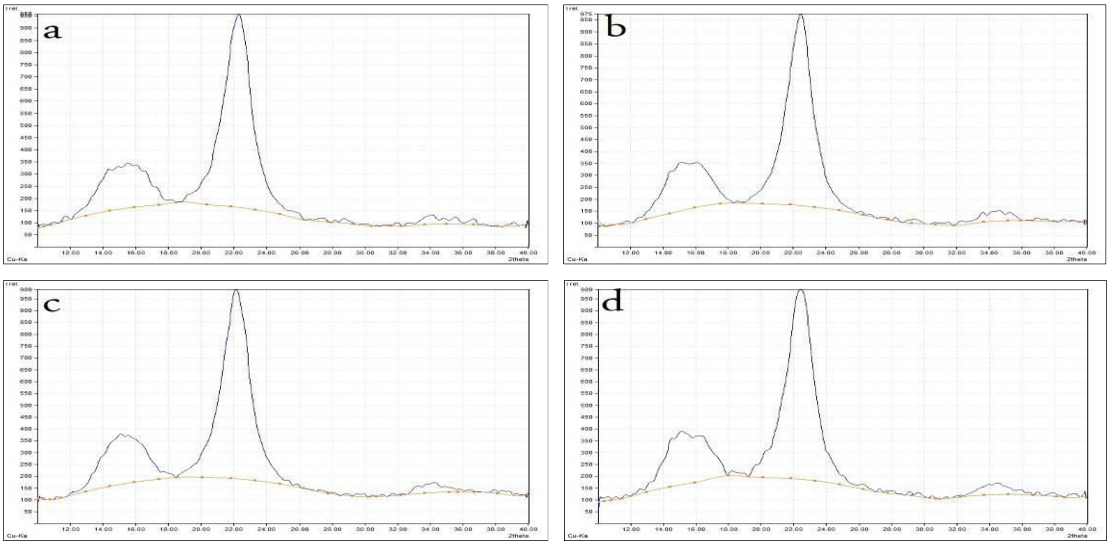

Figure (13) Shows X-ray diffractograms of chemical pulp paper studied before and after ageing, (a) control, (b) aged at 105 ˚C,(c) aged at 130 ˚C & (d) at 150 ˚C.

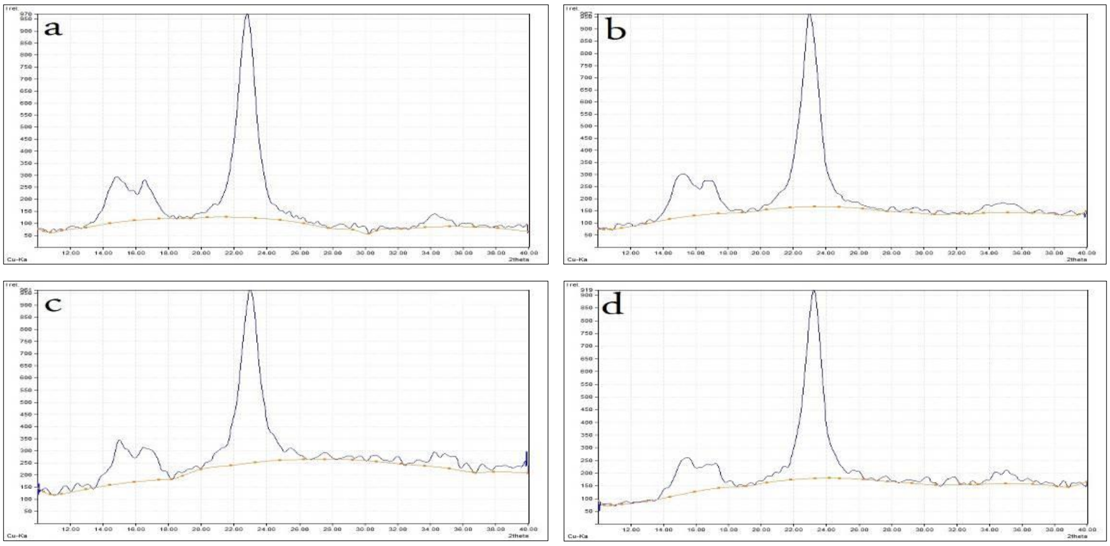

Figure (14) Shows X-ray diffractograms of mechanical pulp paper studied before and after ageing, (a) control, (b) aged at 105 ˚C, (c) aged at 130 ˚C & (d) at 150 ˚C.

Table (2) crystalline Index of different aged paper (30 days thermal ageing 105 ˚C, 130 ˚C & 150 ˚C

Samples	**Crystalline area**		**Amorphous area**		**Crystallinity index (%)**
	2θ (˚)	***Counts***	***2θ (˚)***	***Counts***	
Un aged cotton	22.6	850	19.0	165	80.6
Aged cotton (105˚C)	22.53	950	18.4	200	78
Aged cotton (130˚C)	22.52	795	18.4	140	82
Aged cotton (150˚C)	22.52	860	18.3	170	80
Un aged mechanical pulp	22.61	775	18.5	175	77
Aged mechanical pulp (105˚C)	22.5	580	18.40	148	74
Aged mechanical pulp (130˚C)	22.52	650	18.30	230	63
Aged mechanical pulp (150˚C)	22.52	450	18.40	155	68
Un aged chemical pulp	22.62	875	18.30	175	80
Aged chemical pulp (105˚C)	22.62	800	18.35	175	80
Aged chemical pulp (130˚C)	22.63	850	18.30	225	73
Aged chemical pulp (150˚C)	22.61	975	18.35	225	76

4. Discussion

The micrographs showed differences in paper degradation patterns & paper types between different temperatures under this study. The results proved that higher temperature serves two distinct roles: the first, it increases the rate of evaporation. The second one is it increasing molecular mobility without structural rearrangements. Furthermore, the results proved that this structure is formed in glucose chains of two adjacent pearls on a string structure due to chemical cleavage of the glucose chains and de-cross linking. It is probably one of the breakdown structures of the physical unwinding of fibrils and fibres at higher structural levels, the chemical changes of paper surfaces had greater effect on the changes during heat ageing. As revealed in SEM results, the changes occurring due to ageing in the structure of heat-treated paper tested in this study might be attributed to the surface structural changes cracks present on heat-treated sample surfaces after artificial ageing. Moreover, it was found that the heat causes additional hornification relative to removing the water at room temperature. Higher temperatures also promote a change from elastic to plastic deformation in cellulose pore structure and the rate and temperature of drying can influence the overall value of hornification. Within the same context, the FTIR study proved that explicit changes in spectra of the degraded samples of cotton occurred in the region between 1400 cm-^{1}and1300 cm-^{1}. Three bands at 1372 cm-^{1}, 1335 cm-^{1} and 1316 cm-^{1} occur due to COH and HCC bending vibrations, where, the bands at 1372 cm-^{1} and 1335 cm-^{1} are typical of crystalline cellulose$^{.}$ Moreover, a band at 1372 cm^{1} loses its intensity due to ageing; it becomes weaker due to larger amount of the amorphous cellulose. Finally, at chemical pulp the band at 1430 cm-^{1} is assigned as “crystalline” and the band at 897 cm-^{1} as “amorphous”. A relative shift in the band at 1430 cm-^{1} from higher to lower frequencies is observed, this is a sign of the degradation processes of the cellulose especially at 150 ˚C. Crystallinity is thought to be an important factor in determining mechanical properties such as stiffness or strength because highly ordered material is less able to absorb energy by deformation. If there is significant hydrogen bonding or cross linking, there may be an associated increase in ordering which could be detected using crystallinity measures. The assumption of a two phase system (crystalline and amorphous) is only a rough approximation, which means that small or imperfect structural rearrangements may not be detected.

Conclusions

The thermal characteristics of three types of paper decay by heat ageing at 105,130 & 150 ˚C were investigated using SEM, FTIR and XRD. The conclusions that can be reached from this investigation can be summarized as follows: ***** *It was found that the chemical pulp is more resistant to heat ageing than the cotton and mechanical pulp in the early stages (102 ˚C) & at 150 ˚C, this can be interpreted as, the high temperature accelerates the rate of degradation because it accumulates in the degraded parts of the cell walls and take their place which increases the degradation. Finally, we can say that heat degrade paper types resulting in a gradual breakdown of paper structure.* ***** *It should be noted that during shrinkage some bundles split and wind up and turn into thinner fibres, which in some cases made it impossible to measure the same fibres during the whole shrinkage process from start to end by SEM.* ***** *Significant changes in IR spectra confirmed that higher temperature serves two distinct roles: first, it increases the rate of evaporation, and secondly it increases molecular mobility without structural rearrangements.* ***** *The rigidity of cellulose fibers increases and their flexibility decreases with increasing ratio of crystalline to amorphous regions starting from 105 ˚C.*

Acknowledgment

The author gratefully acknowledge to Dr Adel Bayoumy ,Scanning Electron Microscope Laboratory, the Egyptian Mineral resources authority Central Laboratories Sector, the ministry of petroleum, Cairo, Egypt, for his technical assistance during this research.

References

[1] Hiltunen, M., (2013). *Cellulose based graft copolymers prepared via controlled radical polymerization methods,* Ph.D., Laboratory of Polymer Chemistry, Department of Chemistry, Helsinki Univ., Finland.

[2] Heinze, T. & Liebert, T., (2001). Thermal degradation of wood components, *Progress Polymer Society*, Vol. 3 (26), pp: 1689-1762.

[3] Raj Bogati D., (2011). *Cellulose based biochemical and their application*, Bachelor’s Thesis, Faculty of Technology, Saimaa Univ. of Applied Sciences, France.

[4] Bielecki, S., Krystynowicz, A., Turkiewicz, M. & Kalinowska, H, (2005). Bacterial cellulose, in: Steinbüchel, A. & Doi, Y. (eds.) *Biotechnology of polymer: From synthesis to patents*, Wiley-VCH, Verlag GmbH & Co, Germany, pp: 381-434

[5] Jonas, R. & Farah, L., (1998). Production and application of microbial cellulose. *Polymer Degradation and Stability*, Vol. 59, pp: 101-106.

[6] Michaelsen, A., Pinzari, F., Barbabietola, N. & Piñar, G., (2013). Monitoring the effects of different conservation treatments on paper-infecting fungi, *Int. Biodeterioration & Biodegradation*, Vol. 84, pp: 333-341.

[7] Kavkler, K., Cimerman, N., Zalar, P. & Sar, A., (2011). FTIR spectroscopy of biodegraded historical textiles, *Polymer Degradation and Stability,* Vol. 96, pp: 574-580.

[8] Kotowa, S., (2004). Biodeterioration of textiles. *Int. Biodeterioration & Biodegradation*, Vol. 53, pp: 165-170.

[9] Kato, K. & Cameron, R., (1999). A review of the relationship between thermally-accelerated ageing of paper and hornification, *Cellulose,* Vol. 4 (6), pp: 23-40.

[10] Ohsawa, N. & Okagawa, J., (1989). How to see interfibre bonding in paper sheets. *J. of Pulp Paper Science*, Vol. 15 (1), pp: 17-22.

[11] Fernando, D. & Daniel, G., (2004). Micro-morphological observations on spruce TMP fibre fractions with emphasis on fibre cell wall fibrillation and splitting. *Nord. Pulp Paper Res*. J, Vol. 19 (3), pp: 278-285.

[12] Agrawal, P. & Barkeshli, M., (1997). *Conservation of books, manuscripts and paper documents,* Indian Council of Conservation Institutes, Lucknow, India.

[13] Mackay, G., (1967). *Mechanism of thermal degradation of Cellulose: A review of the literature*, Forestry Branch Departmental Publication, Canada.

[14] Figen, A., Terzi, E., Yilgör, N., Kartal, S. & Pişkin, S., (2013). Thermal degradation characteristic of Tetra Pak panel boards under inert atmosphere, *Korean J. Chem. Eng.*, Vol. 30 (4), pp: 878-890

[15] Kondo, T., (1997). Studies on thermal degradation of cellulosic fibers treated with flame retardants, *J. of Polymer Science*, Vol. 35, pp: 717-723.

[16] Jablonský, M., Botková, M., Šutý, Š., Šmatko, L. & Šima, J., (2014). Accelerated ageing of newsprint paper: Changes in swelling ability, WRV and electro kinetic properties of fibres, *Fibres & Textiles in Eastern Europe*, Vol. 22 (2), pp: 108-113.

[17] Stamm, J. (1956). *Thermal degradation of wood cellulose*, Dover Publications NY.

[18] Madorsky, L., (1964). *Thermal degradation of organic polymers*, Interscience Publishers, NY.

[19] Tesoro, G., (1976). Current research on chemical modification of cellulose, *Pure & Applied Chemistry,* Vol. 46, pp: 239-245.

[20] Barański, A., Dziembaj, R., Konieczna-Molenda, A., Łagan, J., Walas, S., (2004). On the applicability of arrhenius equation to accelerated ageing tests. The case of alum-impregnated cellulose, *Polish J. of Chemical Technology*, Vol. 6, pp: 1-8

[21]Jablonsky, M., Katuscak, S., Holúbková, S., Hrobonova, K. & Lehotay, J., (2011). The effect of acetic and formic acid formation during accelerated ageing on embrittlement of newsprint paper, *J. Restaurator*, Vol. 32 (4), pp: 318-347

[22] ISO 5630-1:1991, (1991). *Paper and board - accelerated ageing - Part 1: dry heat treatment at 105 ˚C*, International Organization for Standardization, Geneva.

[23] ISO 5630-4:1986, (1986). *Paper and board - accelerated ageing - part 4: dry heat treatment at 120 or 150 ˚C*, International Organization for Standardization, Geneva.

[24] Segal, L., Creely, J., Martin, A. & Conrad, C., (1959). An empirical method for estimating the degree of crystallinity of native cellulose using the X-ray diffractometer, *Textile Research Journal*, Vol. 29 (10), pp: 786-794.

[25] Segal, L., Loeb, J. & Creely, J., (1984). An X-ray study of the decomposition product of the Ethylamine-cellulose complex, *J. of Polymer Science*, Vol. 13 (69), pp: 193-206.

[26] Lewin, M. & Roldan, G., (1971). The effect of liquid anhydrous ammonia in the structure and morphology of cotton cellulose, *J. of Polymer Science*, Vol. 36, pp: 213-229.

[27] Christensen, P. & Giertz, H., (1966). The cellulose-water relationship, in: Bolam, F. (ed.) Proceedings of a Symposium Organized by BPBMA, London. pp: 59-89

[28] Derrick, R., Stulik, D. & Landry, M., (1999). *Infrared spectroscopy in conservation science*, the Getty Conservation Institute, Los Angeles.

[29] Hinterstoisser, B. & Salmén, L., (2000). Application of dynamic 2D FTIR to cellulose, *Vibrational Spectroscopy*, Vol. 22 (1-2), pp: 111-118.

[30] Alia, M., Emsley, A., Herman, H. & Heywood, R., (2001). Spectroscopic studies of the ageing of cellulosic paper, *Polymer*, Vol. 42 (7), pp: 2893-2900.

[31] Pandey, K. & Pitman, J., (2003). FTIR studies of the changes in wood chemistry following decay by brown-rot and white-rot fungi, *Int. Biodeterioration & Biodegradation*, Vol. 52 (3), pp: 151-160.

[32] Hergert, H., (1960). Infrared spectra of Lignin and related compounds. II. Conifer Lignin and model compounds, *J. Org. Chem.*, Vol. 25 (3), pp: 405-413

[33] Pandey, K. & Theagarajan, K. (1997). Analysis of wood surfaces by DRIFT & photo acoustic (PAS) Fourier transforms infrared spectroscopic techniques, *Holz als Roh- und Werkstoff*, Vol. 55 (6), pp: 383-390.

[34] Łojewska, J., Lubańska, A., Łojewski, T., Miśkowiec, P. & Proniewicz, L. (2005). Kinetic approach to degradation of paper: situ FTIR transmission studies on hydrolysis and oxidation, *e-Preservation Science*, Vol.2, pp: 1-12.

[35] Hassan, M., Rowell, R., Fadl, N., Yacoub, S. & Christiansen, A., (2000). Thermoplasticization of bagasse. I. preparation and characterization of esterified bagasse fibers, *J. of Applied Polymer Science*. Vol. 76, pp: 561-576.

[36] Weise, U., Maloney, T, & Paulapuro, H., (1996). Quantification of water in different states of interaction with wood pulp fibres. *Cellulose*, Vol. 3 (4) pp: 189-202.

[37] Robertson, A., (1963). The physical properties of wet webs: 2. Fibre properties and wet web behaviour, *Svensk PappTidn*., Vol. 66 (12), pp: 477-497.

[38] Poletto, M., Pistor, V., Zeni, M. & Zattera, A. (2011). Crystalline properties and decomposition kinetics of cellulose fibers in wood pulp obtained by two pulping process, *Polymer Degradation and Stability*, Vol. 96 (4), pp: 679-685.

[39] Oh, S., Yoo, D., Shin, Y. & Seo, G; (2005). FTIR analysis of cellulose treated with sodium hydroxide and carbon dioxide. *Carbohydrate Research*, Vol. 340 (3), pp: 340-417.

[40] Proniewicz, L., Paluszkiewicz, C., Wesełucha-Birczyńska, A., Majcherczyk, H., Barański, A. & Konieczna, A., (2001). FT-IR and FT-Raman study of hydrothermally degradated cellulose. *J. Mol Struct*, Vol. 596 (1-3), pp: 163-169.

[41] Kavkler, K., Gunde-Cimerman, N., Zalar, P. & Demšar, A., (2011). FTIR spectroscopy of biodegraded historical textiles, *Polymer Degradation and Stability*, Vol. 96 (4), pp: 574-580

[42] Garside, P. & Wyeth, P. (2003). Identification of cellulosic fibres by FTIR spectroscopy: thread and single fibre analysis by attenuated total reflectance, *Studies in Conservation*, Vol.48 (4), pp: 269-275

[43] Leschine, S., (1995). Cellulose degradation in anaerobic environments Microbial *Annu Rev Microbiol.*, Vol. 49, pp: 399-426.

[44] Ziabicki, A. (1976). *Fundamentals of fibre formation: The science of fibre spinning and drawing*, John Wiley & Sons, London.

[45] Eriksson, K., (1985). Fungal degradation of wood components, *Pure and Applied Chemistry*. Vol. 53 (1), pp: 33-43,